

POLYMER COMBUSTION AND NEW FLAME RETARDANTS

by

**T. Kashiwagi, J.W. Gilman, M.R. Nyden
Building and Fire Research Laboratory
National Institute of Standards and Technology
Gaithersburg, MD 20899, USA**

Reprinted from the 6th European Meeting on Fire Retardancy of Polymeric Materials (FRPM'97), September 24-26, 1997. Organised jointly by the 'Laboratoire de Chimie Analytique et de Physico-Chimie des Solides' de l'E.N.S.C. de Lille and the 'Centre de Recherche et d'Etude des Procédés d'Ignifugation des Matériaux' at her University of Lille (France). Proceedings. Special Publication No. 224. The Royal Society of Chemistry, Thomas Graham House, Science Park, Milton Road, Cambridge CB4 4WF, UK, 1998.

NOTE: This paper is a contribution of the National Institute of Standards and Technology and is not subjected to copyright.

T. Kashiwagi, J. W. Gilman, M. R. Nyden,

Building and Fire Research Laboratory, National Institute of Standards and Technology
Gaithersburg, MD 20899 USA

S. M. Lomakin

Guest researcher from Institute of Biochemical Physics,
Russian Academy of Sciences, Moscow, Russia

1. INTRODUCTION

A majority of polymer-containing end products (for example, cables, carpets, furniture) must pass some type of regulatory fire test to help assure public safety. Thus, it is important to understand how polymers burn and how to best modify materials to make them less flammable in order to pass such tests without compromising their uniquely valuable physical properties and also significantly increasing the cost of end products. This paper briefly describes chemical and physical processes occurring in the gas and condensed phases during the combustion of polymers and methods to reduce their flammability.

Combustion of polymer materials is characterized by a complex coupling between condensed phase and gas phase phenomena. Characteristics of the critical role in each phase are briefly described below.

1.1. Condensed Phase

In order to burn a polymeric material, thermal energy must be added to it to raise its temperature sufficiently to initiate degradation. This energy could be from an external source, in the case of an ignition event such as a match, or from an adjacent flame as heat feedback in the case of flame spread and burning. Thermal radiation is the primary mode of energy transfer from the flame to the polymer surface as discussed later except for small samples (roughly less than 15 cm diameter).

When temperatures near the surface become high, thermal degradation reactions occur and these evolve small gaseous degradation products. The majority of the evolved products from polymers is combustible. Depending on the nature of the polymer, thermal degradation

reactions may proceed by various paths. Since there are several excellent books and articles describing thermal degradation chemistry in detail¹⁻³, only an extremely brief discussion is presented here. It has been accepted that the majority of vinyl polymers degrade thermally by a free radical chain reaction path. Free radical chain reactions consist of random or chain-end initiated scission, depropagation, intermolecular or intramolecular transfer, and termination reactions. Polyethylene, PE, is a typical example of a polymer that undergoes scission at random locations on the main chain to yield many smaller molecular fragments. Polystyrene, PS, polypropylene, PP, and polymethylacrylate, PMA, belong to this group. Polymethylmethacrylate, PMMA, undergoes a reversal of the polymerization reaction after the initial breakage and yields mainly monomer molecules. Polyoxymethylene, poly- α -methystyrene, and polytetrafluoroethylene belong to this group. These two groups of polymers undergo almost complete degradation while leaving hardly any char (carbonised polymer residue). Polymers with reactive side groups attached to the backbone of a polymer chain may degrade initially as a result of interactions or instabilities of these groups; such reactions may then lead to scission of the backbone. Polyvinylchloride, PVC, and polyvinyl alcohol, PVA, are examples of such polymers. This group tends to undergo cyclization, condensation, recombination or other reactions which ultimately yield some char. Diene polymers, polyacrylonitrile, and many aromatic and heterocyclic backbone polymers also belong to this char-forming group. Common to the pyrolysis of all these polymers is the formation of conjugated multiple bonds, transition from a linear to a cross-linked structure, and an increase of the aromaticity of the polymer residue⁴. For polymers containing aromatic carbon- and/or heterocyclic links in the main chain of the polymer structure, general features of their pyrolysis and char yield have been derived^{5,6}.

As described above, the type of polymer structure, thermal properties, and the amount of heat transferred to the polymer determine the depth over which the polymer is heated sufficiently to degrade. Since the boiling temperatures of some of the degradation products are much less than the polymer degradation temperatures, these products are superheated as they form. They nucleate and form bubbles. Then, these bubbles grow with the supply of more small degradation products by diffusion from the surrounding molten polymer⁷. Since the polymer temperature is higher near the surface than deeper, the polymer sample is more degraded there and its molecular weight, M , is lower. Since the viscosity of the molten polymer, η , depends strongly on molecular weight and temperature (for example⁸, $\eta = cM^{3.4}$

or $\eta = \exp\{-M/(E(T-T_g))\}$, the viscosity near the surface is much less than that in the interior. The net result is a highly complex generation and transport of bubbles containing small molecules from the interior of the polymer melt outward through a strong viscosity gradient that heavily influences bubble behavior. A qualitative description of this complex transport process and its effect on gasification rate has been previously given⁹.

The transport of the degradation products through the molten polymer layer near the surface is not well understood. Understanding of transport processes is important if intumescent char layer or barrier layer formation is used as a flame retardant approach. Very little study has been conducted to understand these transport processes except a capillary transport study through a well-controlled char layer¹⁰.

1.2. Gas Phase

The heat release rate is one of the key quantities characterising the hazard of a material. However, the heat from oxidation reactions in a flame is released in two components; one is convective and the other is radiative. The fraction of each component, the convective fraction X_c and the radiative fraction X_r (normalised by the idealised heat of combustion of the material), depends strongly on the chemical structure of the material. Typical results for a pool flame configuration as a function of fuel mass flux are shown in Figure 1 and Figure 2 for methane (and natural gas) and acetylene, respectively¹¹. The term X_1 is the fraction of the idealised heat release, which is fed back to the fuel surface. In these flames, the flame becomes taller and larger with an increase in mass flux.

For large size methane (and natural gas) flames, roughly 80% of the heat release is convected away and roughly 20% of the heat release is radiated. A small fraction, about 2-3% of the total heat release, is fed back to the fuel surface. However, for small flames, the radiative fraction of the heat release becomes quite small due to the smaller flame size and the feedback fraction, X_1 , increases. For acetylene flames, the radiative fraction increases up to slightly above 30% and the convective fraction decreases to as low as 45%. Combustion efficiency, X_a (the measured chemical heat release ($X_c + X_r$) divided by the idealised heat release), decreases to about 65% with an increase in the fuel mass flux. Unsaturated materials and aromatic materials tend to have similar characteristics as acetylene and their radiative fraction tends to be between 30 and 40% due to an increase in soot particle concentration in their flames. These results show clearly that heat release characteristics and heat feedback

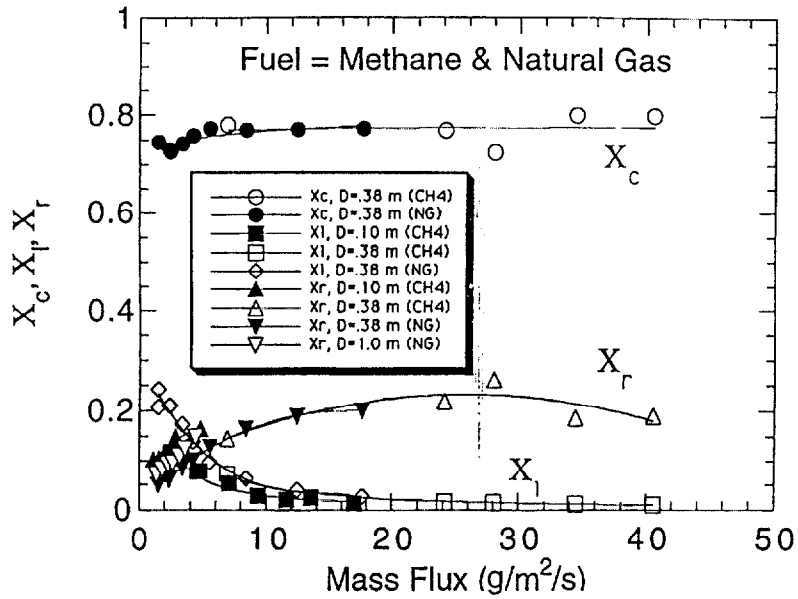


Figure 1. Fractions of idealised heat release dissipated by convection (X_c), radiation (X_r) and feedback to the fuel surface (X_i) with respect to fuel mass flux.

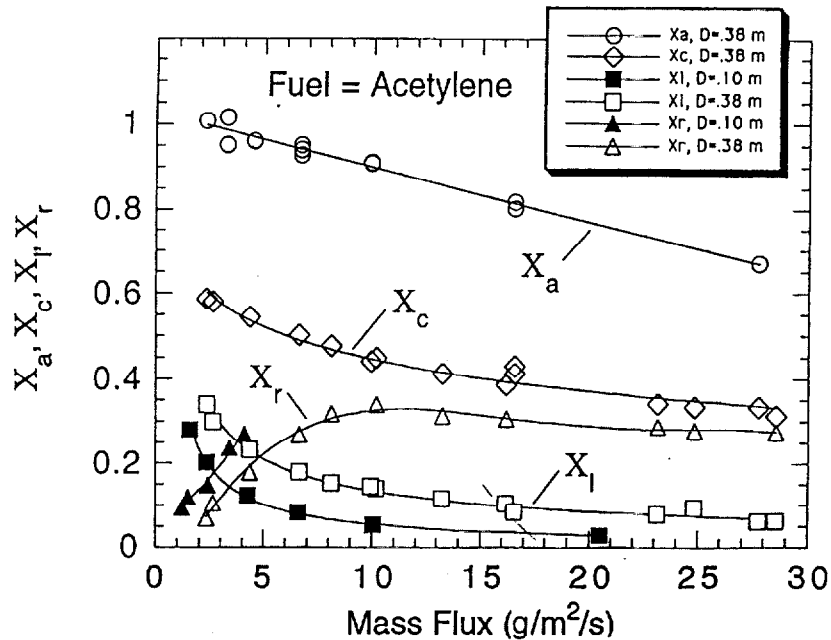


Figure 2. Fractions of idealised heat release dissipated by convection (X_c), radiation (X_r) and feedback to the fuel surface (X_i) with respect to fuel mass flux, X is combustion efficiency.

rates depend not only on the chemical structure of the materials but also the diameter of a pool flame and the fuel mass flux.

Radiation from the flame to the sample surface is a major heat feedback mode when the diameter of a pool flame becomes large (roughly more than 15 cm). The radiant flux from flame to the sample surface was measured using a miniature radiant flux gauge at the surface of 30 cm diameter methanol, heptane, and toluene pool flames¹². Although the methanol flame is blue and does not generate soot particles, there is still a significant amount of radiative feedback by CO₂ and H₂O band emissions. The radiative heat feedback has a non-uniform spatial distribution. The fraction of radiation in the total heat feedback is about 80% at the center and gradually decreases to about 10% at the edge of the methanol pool flame as shown in Figure 3. In this figure, the radiative component of heat feedback flux, Q_r , is Normalized by the local net heat feedback flux, Q . For the sooty toluene flame, however, this fraction is nearly constant (about 100%) across the pool surface¹². It appears that the radiative feedback flux from a pool flame might not increase with pool diameter beyond a certain size due to absorption of radiation from the flame to the fuel surface by the vaporised fuel and particulates near the pool surface¹³.

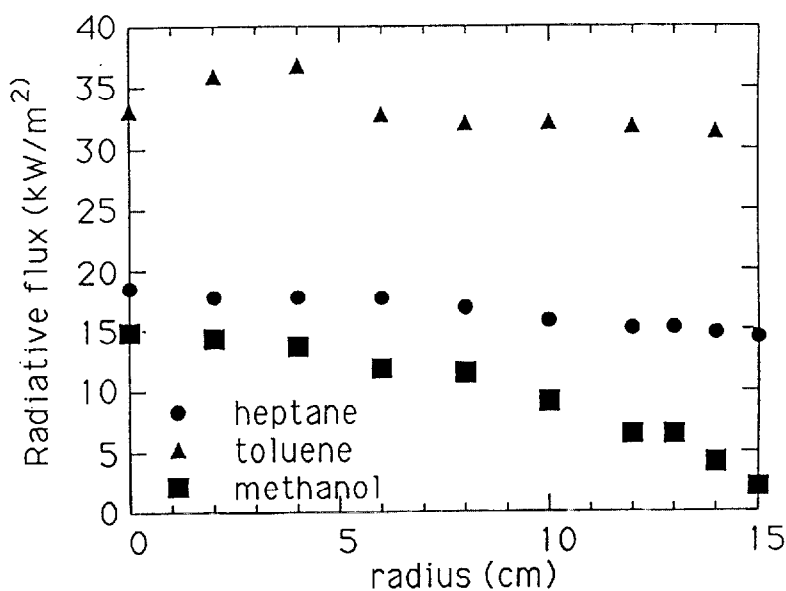


Figure 3. Measured radial radiative feedback rate distribution for 30 cm diameter pool flames with three different liquid fuels.

2. FLAME RETARDANTS

The fire safety of materials can be enhanced by increased ignition resistance, reduced flame spread rates, lesser heat release rates and reduced amounts of toxic and smoke products, preferably simultaneously within reasonable costs.

The most practical approach to enhance fire safety performance is the use of flame retardant additives to inexpensive and large volume commodity polymers such as PE, PP, PS, PVC, and so on. Unfortunately, the majority of these polymers have low to medium thermal stability and high heat of combustion. The additives must have a minimum impact on physical properties and product cost. Although halogenated flame retardants generally lower the heat of combustion and reduce the heat feedback rate from a flame to the polymer surface and are highly effective for reducing the heat release rate of commodity polymers, the future use of these retardants is unclear. Public perception of the environmental impact of combustion of certain halogenated flame retardants during incineration has become an issue in Europe^{14,15}.

Although there are many possible approaches to non-halogenated flame retardancy such as the use of aluminum trihydrate or magnesium hydroxide (both generate significant amount of water during degradation and act as a heat sink). Another approach is the formation of char. There are three mechanisms whereby the formation of char reduces flammability: (1) part of the carbon (and hydrogen) stays in the condensed phase, thus reducing the amount of gaseous combustible degradation products evolved; (2) the low thermal conductivity of the char layer over the exposed surface acts as thermal insulation to protect the virgin polymer beneath¹⁶; and (3) a dense char acts as a physical barrier to gaseous combustible degradation products¹⁷.

The majority of commodity polymers do not form char during their combustion. This char forming approach is most successful if the polymer chars rapidly and early in the burning process. To be useful the charring process must be designed so that it occurs at a temperature greater than the processing temperature but before the polymer decomposition has proceeded very far. The physical structure of char has significant effects on polymer flammability. It is generally preferable to form an intumescent char (swollen char) having a cellular interior structure consisting of pockets of trapped gas¹⁸. The dominant protective role of an intumescent char is mainly via its thermal insulating capability^{17,18} rather than an obstacle to the passage of volatile and low-viscosity products into the gas phase because low-viscosity

polymeric melts can rise through an intumescent char layer due to capillary forces¹⁰.

One possible such approach is the use of phosphorous based compounds whose effective flame retardant performance is well known^{19,20}. However, it appears that the mechanism of flame retardancy depends on the polymer resin and the type of phosphorus compounds. It has been reported that the flame retardant operates in the condensed phase by forming char for rigid polyurethane²¹ but, for polystyrene, phosphorous flame retardants act primarily in the gas phase²². The use of phosphorous compound was extended to determine flame retardant effectiveness of phosphine oxides, various hydrolytically stable aromatic phosphine oxides were chemically incorporated into nylon 6,6, PET, and epoxy polymers.

2.1. Phosphine Oxide

All phosphine oxide copolymers were synthesised by J. McGrath's group at Virginia Polytechnic Institute and State University and the synthetic methods used are described in refs. 23-25. Samples were prepared by compression molding and their size was 10 cm square with about 3 mm thickness. The flammability properties of these samples were measured by the Cone Calorimeter (ASTM E1354) at external flux of either 35 kW/m² or 40 kW/m² in air. The sample was wrapped in a thin aluminum foil except the irradiated sample surface and mounted horizontally on a calcium silicate board as an insulation material. A heavy metal container used in the standard test procedure was not used in this study to avoid heat loss to the container. The effect of incorporation of triphenylphosphine oxide, TPO, into nylon 6,6 as a copolymer on the heat release rate per unit surface area is shown in Figure 4 for three different levels of phosphine oxide from 10 mol. % to 30 mol. %. A significant decrease in heat release rate is observed as the amount of the TPO co-monomers is increased. Piloted ignition delay time decreases slightly with increasing amount of the TPO. This is consistent with the slight decrease in the onset of thermal degradation temperature (from 410°C for nylon 6,6 to 402°C for the 30 mol. % of the phosphine oxide sample²⁴) seen in the TGA data (thermal gravimetric analysis) in air. The mass burning flux is calculated from the transient sample weight loss rate divided by the initial sample surface area and the results are shown in Figure 5. The mass loss flux decreases with the amount of TPO, but this trend is much less than that of the heat release rate. The heat of combustion, ΔH_c , is calculated from the transient heat release rate divided by the transient mass loss rate at the same instance. The ΔH_c results shown in Figure 6 indicates that the heat of combustion decreases with increase in TPO. A reduction in the heat of

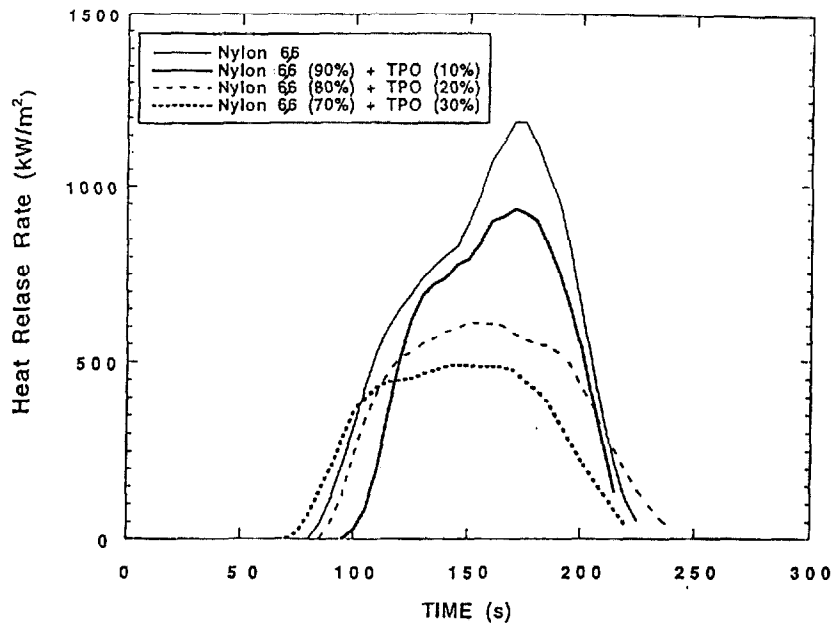


Figure 4. Comparison of heat release rate per unit surface area of nylon6,6 and copolymer samples of nylon6,6/TPO at external flux of 40 kW/m².

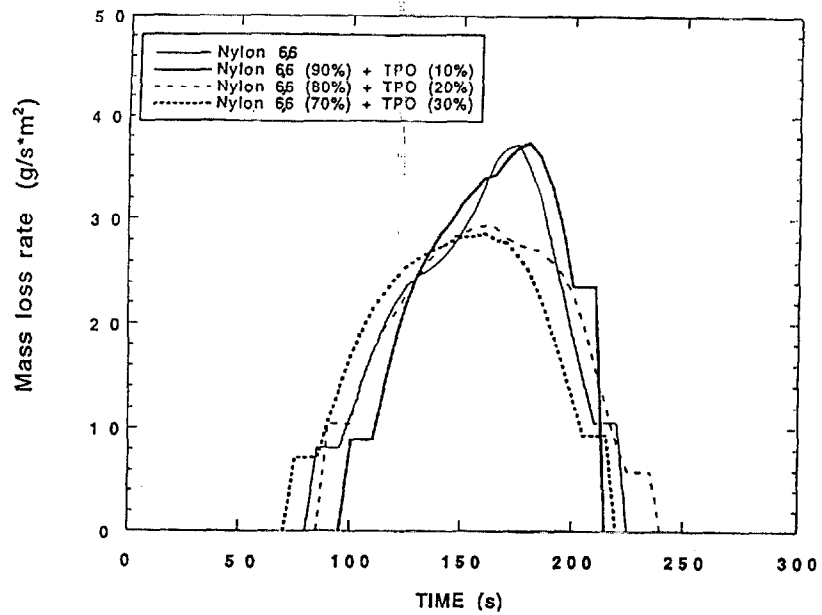


Figure 5. Comparison of mass loss rate per unit surface area of nylon6,6 and copolymer samples of nylon6,6/TPO at external flux of 40 kW/m².

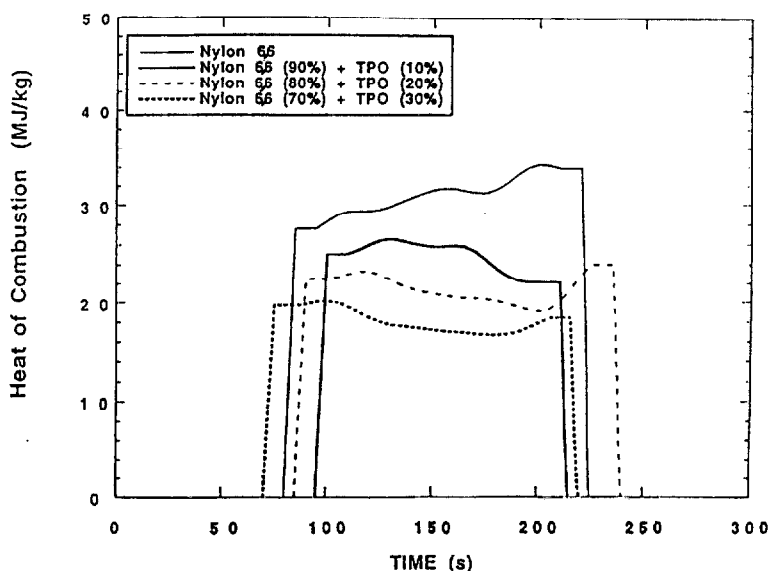


Figure 6. Comparison of specific heat of combustion of nylon6,6 and copolymer samples of nylon6,6/TPO at external flux of 40 kW/m^2 .

combustion is about 40% from nylon 6,6 to the copolymer of TPO (30 mol. %) and nylon 6,6. However, the yield of char after the test is from $2.3 \pm 0.2 \%$ for nylon 6,6 to $8.7 \pm 0.8 \%$ for the copolymer sample. These trends indicate that there is some flame retardant activity in the condensed phase but it appears that the majority of the flame retardant activity is in the gas phase. This is confirmed by significant increases in specific extinction area, shown in Figure 7.

The specific extinction is calculated from the extinction measurement of a He-Ne laser beam passing through the exhaust duct of the Cone Calorimeter divided by the volume flow rate in the duct and the transient mass loss rate. This value indicates the concentration of soot particulates generated by the combustion of the sample. Since the effect of the TPO on the mass loss rate is relatively small, as shown in Figure 5, the overall rate of CO and soot particles formation increased with an increase in the phosphine oxide content in the copolymer sample.

The flammability properties of these samples are summarised in Table 1. A small increase in char yield (from 0 % to 8.5 %) with an increase in the TPO is also observed in the TGA study at 750°C^{24} . Although the physical properties of the copolymer tends to be better

than that of the blended sample, the cost of the copolymer sample might be higher than that of the blended sample. Another flammability study was carried out to compare the flame retardant effectiveness of the copolymer and a blend material. TPO (10 mol. %) was blended with nylon 6,6 and the flammability properties of this blend are compared with those of nylon 6,6 and of the nylon 6,6/TPO copolymer. The comparison of heat release rate among the three samples is shown in Figure 8. The heat release rate of the blended sample does not differ significantly from that of the copolymer but the ignition delay time of the blended sample tends to be shorter than that for the copolymer sample. There are no significant differences in burning rate, heat of flammability properties of nylon 6,6 with TPO as a blend or as a copolymer are not significantly different. Other copolymers based on polycarbonate, PET, and epoxy (Epon 828) with TPO were synthesised to examine the effects of polymer chemical structure on flame retardant effectiveness of the phosphine oxide. The results are similar to those for nylon 6,6. The heat release rates of these polymers are reduced by the incorporation of TPO as a copolymer but an increase in the amount of CO and soot particulates was also observed.

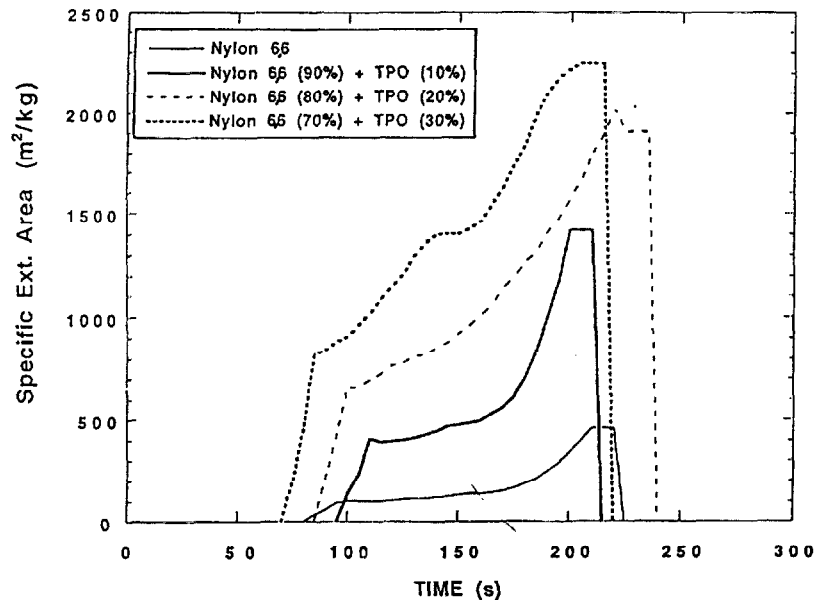


Figure 7. Comparison of specific extinction area of nylon 6,6 and copolymer samples of nylon 6,6/TPO at external flux of 40 kW/m^2 .

The increase in the formation of soot particulates and CO, by the incorporation of TPO, could be caused by the combustion of pendant benzene groups from TPO. When benzene is a part of the polymer backbone, it tends to participate in formation of char⁵. However, pendant benzene groups do not always promote char formation. This is the case in polystyrene where the pendant benzene groups tend to generate soot particulates instead of char. In order to confirm this hypothesis, a new copolymer sample was synthesised with the pendant benzene replaced with methyl.

Sample	Peak heat release rate (kW/m ²)	Total heat release (MJ/m ²)	Heat of combustion (MJ/kg)	Char yield (%)	CO yield (%)	Specific extinction area (m ² /kg)
nylon 6,6	1190 ± 150	95 ± 10	31 ± 3	2.3 ± 0.2	1.4 ± 0.2	177 ± 30
nylon 6,6+TPO(10 %)	930 ± 120	72 ± 7	25 ± 2	6.1 ± 0.6	10 ± 1.5	700 ± 100
nylon 6,6 + TPO(20 %)	610 ± 90	62 ± 6	21 ± 2	7.5 ± 0.7	15 ± 2	1120 ± 150
nylon 6,6 + TPO(30 %)	490 ± 70	50 ± 5	18 ± 2	8.7 ± 0.8	16 ± 2	1480 ± 200

Table 1. Effects of TPO incorporation on the flammability properties of nylon 6,6 at an external flux of 35 kW/m².

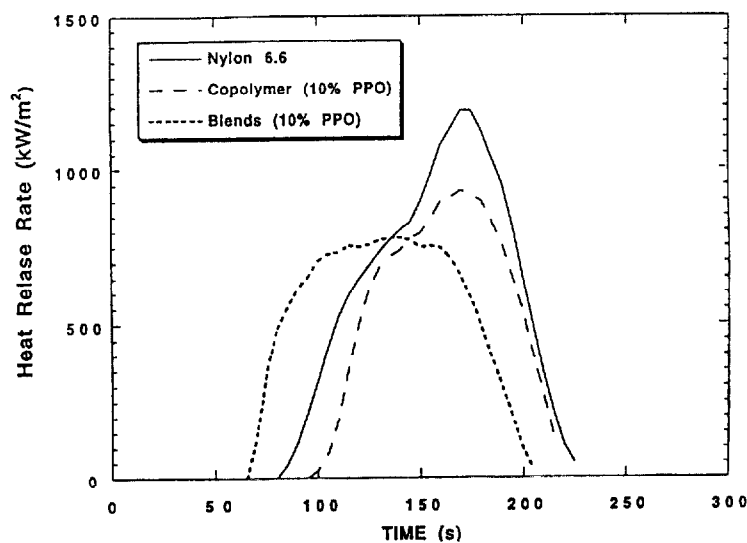


Figure 8. Comparison of heat release rate per unit surface area of nylon6,6, the blended sample and the copolymer sample of nylon6,6/TPO at external flux of 40 kW/m².

The heat release rate of copolymer samples of diphenylphosphine oxide, DPO, with nylon 6,6 is not significantly different from that of copolymer samples of TPO with nylon 6,6 as shown in Figure 9.

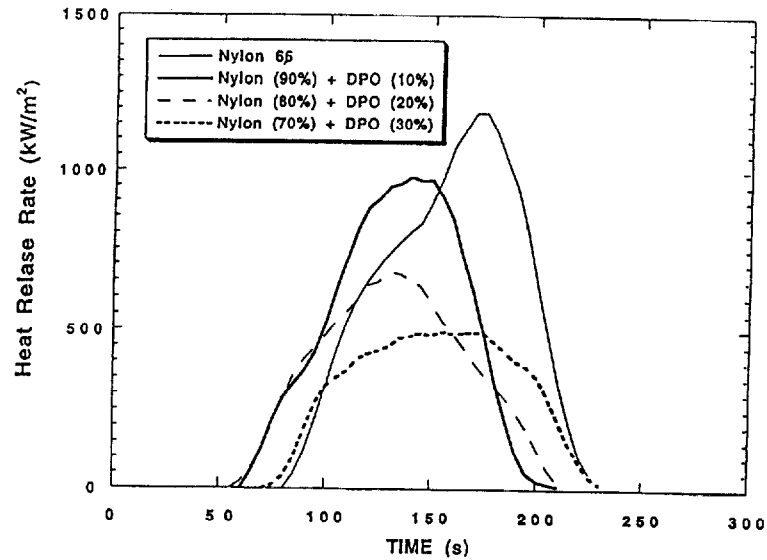


Figure 9. Comparison of heat release rate per unit surface area of nylon6,6 and copolymer samples of nylon6,6/TPO at external flux of 40 kW/m².

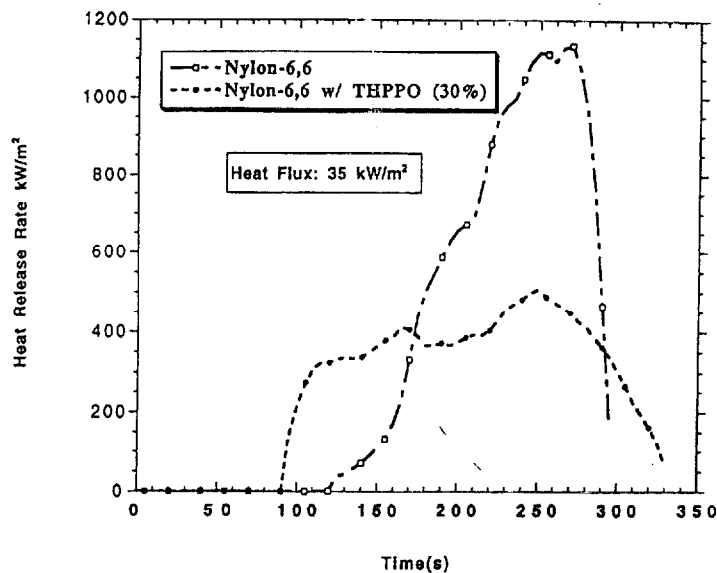


Figure 10. Comparison of heat release rate per unit surface area of nylon6,6 and the nylon6,6/THPPO (30 wt. %) blended samples at external flux of 35 kW/m².

The mass loss rate, heat of combustion, CO yield, and specific extinction area of copolymer samples of DPO/nylon 6,6 are not significantly different from those of copolymer samples of TPO/nylon 6,6.

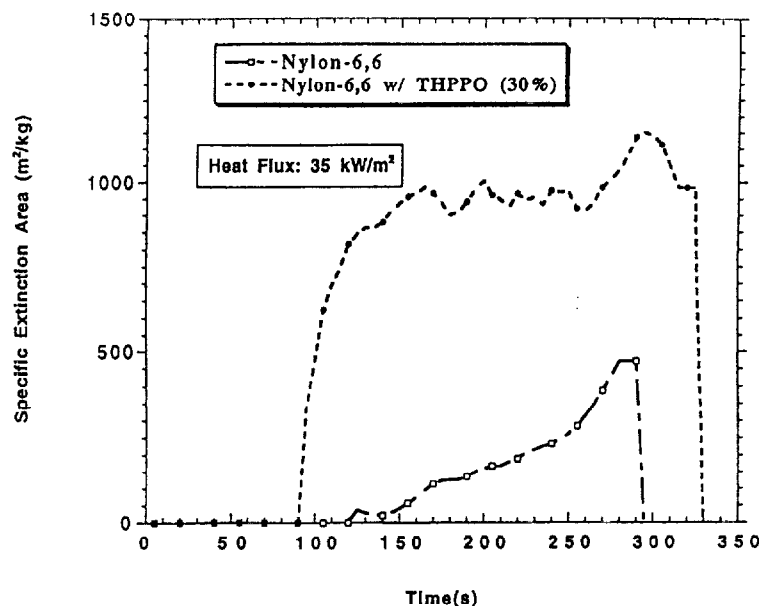


Figure 11. Comparison of specific extinction area of nylon 6,6 and the nylon 6,6/THPPO (30 wt. %) blended samples at external flux of 35 kW/m^2 .

These results indicate that the pendant benzenes do not enhance the formation of CO and soot particulates. To determine if benzene in the copolymer backbone was contributing to the increase in CO and soot particulates, we examined an aliphatic phosphine oxide blended with nylon 6,6. Trihydroxypropylphosphine oxide, THPPO, was used as the aliphatic phosphine oxide. The blended sample has 30 wt. % of THPPO. The heat release rate of the blended sample with THPPO is compared with that of nylon 6,6 sample (This nylon 6,6 is a commercial sample whose thermal degradation characteristics might be different from that of the nylon 6,6 sample used for the copolymer study.). The results, shown in Figure 10 at an external flux of 35 kW/m^2 , show a significant reduction in heat release rate similar to the copolymer samples with TPO. In addition, the specific extinction area of the blended sample is much higher than that of nylon 6,6, as shown in Figure 11. The char yield of the blended

sample was 4.2 %. These results are similar to those of the copolymer samples with TPO. The results suggest that phosphorous is the major factor in controlling the reduction of the heat release rate and the increase in CO and soot particulates. There is evidence which suggests that, if phosphorous is released into the gas phase, then it acts as a radical scavenger of H-atoms^{26,27}.

On the other hand, the measurable char yield in the tested sample suggests that there is some activity in the condensed phase. If phosphorous stays in the condensed phase during combustion, phosphorous could be a significant char forming flame retardant.

2.2. Silica Gel

The intention of using silica gel with K_2CO_3 was to devise a method of in-situ formation of silicon based fire retardants during combustion. The reaction of silica gel and organic alcohols in the presence of metal hydroxides has been shown to give multi-coordinate organosiliconate compounds²⁸. Instead of synthesising these materials and then combining them with various polymers to evaluate their effect on polymer flammability properties, we envisioned the reaction occurring in the condensed phase of the pyrolyzing polymer beneath the burning surface, by combining a polyhydroxylic polymer, e.g. PVA or cellulose, with silica gel and K_2CO_3 . If the reaction between the polymer and the additives occurs, it should crosslink the polymer and might assist in forming a silicon-oxy-carbide, SiOC, type protective char during combustion. The flammability properties of these samples were measured in the Cone Calorimeter at an incident flux of 35 kW/m^2 . The results are summarised in Table 2 for the polymers and polymers with the addition of silica gel and K_2CO_3 ²⁹. Assuming all additives remained in the polymer residue after the test, the char yield was determined as (polymer residue weight - initial additives weight)/initial mass of polymer in the sample. The results show that the additives enhance the formation of carbonaceous char even if the original polymer does not generate any char such as PP, PS and PMMA. The increases in carbonaceous char yield for PVA and cellulose is nearly a factor of 10. It is not surprising that a significant increase in char yield was observed for PVA and cellulose but char was not expected to form for PP and PS which do not have any alcohol groups in their polymer structure. The reduction in peak heat release rate by the additives is quite significant, reaching about 50% for PP, PVA, cellulose, and nylon 6,6. A typical result for the reduction in heat release rate is shown in Figure 12 for PP. However, the heat of combustion is not significantly

affected by the additives and also the concentrations of particulates and CO in the combustion products do not increase with the additives²⁹. These trends are significantly different from those for halogenated flame retardant additives or even for the previously described copolymer samples of phosphine oxide. The results presented here clearly demonstrate that the flammability of a wide variety of polymers is dramatically reduced in the presence of relatively small concentrations of silica gel and K_2CO_3 .

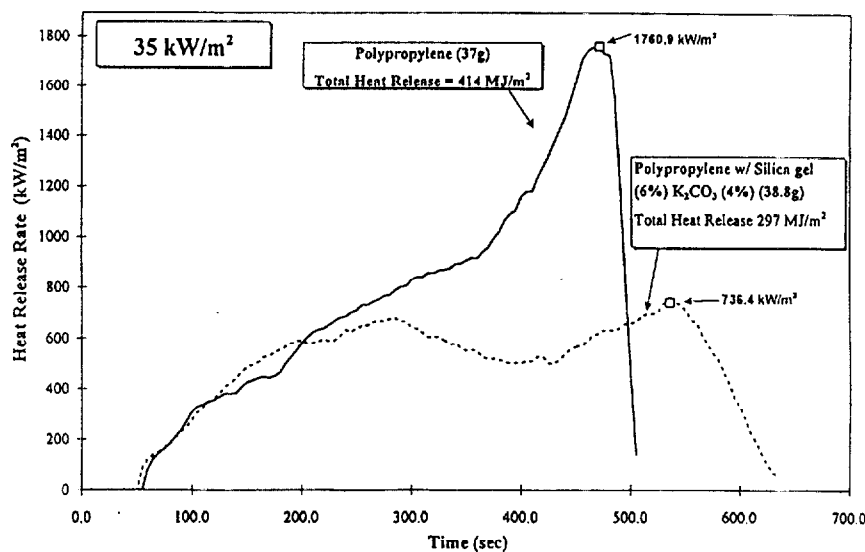


Figure 12. Comparison of heat release per unit surface area of PP and the PP blended sample with silica gel/ K_2CO_3 at external flux of 35 kW/m^2 .

All the data with the addition of silica gel and K_2CO_3 in the polymers described in Table 2 show trends of lower heat release rate, lower sample mass loss rate, and no significant effects on heat of combustion, yields of smoke and CO, and the formation/enhancement of carbonaceous char. These trends show that the site of flame retardancy of the additives is in the condensed phase.

This is more clearly demonstrated by the gasification study of PMMA with the additives in nitrogen²⁹. The PMMA with silica gel and K_2CO_3 (mass ratio of 95:4:1) sample of about 75 cm diameter with about 0.6 cm thickness was exposed to external radiant flux of 41 kW/m^2 in our radiative gasification device.

Sample disk: 75mm x 8mm	Char Yield (%)	LOI (%)	Peak HRR (Δ) (kW/m ²)	Mean HRR (kW/m ²)	Mean Heat of Combustion (MJ/kg)	Total Heat Released (MJ/m ²)	Mean Specific Ext. Area (m ² /kg)	Mean CO yield (kg/kg)
PP	0	-	1,761	803	38	357	689	0.04
PP w/ 6%SG & 4%PC	10	-	736 (58%)	512	33	297	710	0.04
PS	0	18	1,737	1,010	25	277	1,422	0.07
PS w/ 6%SG & 4%PC	6	24	1,190 (31%)	725	25	246	1,503	0.07
PMMA	0	18	722	569	23	319	210	0.01
PMMA w/ 3%SG & 1%PC	15	25	420 (42%)	246	21	231	199	0.05
PVA	4	-	609	381	17	221	594	0.03
PVA w/ 10%PC	9	-	322 (47%)	222	17	145	571	0.03
PVA w/ 10%SG	29	-	252 (57%)	173	15	131	361	0.03
PVA w/ 3%SG & 1%PC	16	-	295 (52%)	232	16	166	447	0.03
PVA w/ 6%SG & 4%PC	43	-	194 (68%)	114	12	101	201	0.03
Cellulose	4	-	310	161	11	101	27	0.02
Cellulose w/ 6%SG & 4%PC	32	-	149(52%)	71	5.3	34	20	0.04
SAN	2	-	1,499	837	25	197	1,331	0.07
SAN w/ 6%SG & 4%PC	3	-	1,127 (25%)	772	23	169	1,301	0.06
Nylon 6, 6	1	30	1,131	640	23	108	234	0.02
Nylon 6, 6 w/ 4%PC	3	-	854 (25%)	570	25	103	342	0.03
Nylon 6, 6 w/ 6%SG	4	-	558 (51%)	365	24	111	164	0.02
Nylon 6, 6 w/ 3%SG & 2%PC	5	33	526 (53%)	390	22	105	171	0.02
Nylon 6, 6 w/ 6%SG & 4%PC	6	30	546 (52%)	370	24	102	185	0.02

Incident heat flux = 35 kW/m²; SG = Silica Gel; PC = K₂CO₃

Table 2. Flammability properties of various polymers with silica gel and potassium carbonate in Cone calorimeter and Limiting Oxygen Index test. Uncertainties in peak heat release rate and in mean extinction area are $\pm 15\%$ and those of other quantities are $\pm 10\%$.

The weight loss rate and gasification behavior of PMMA and PMMA with the additives were recorded by an electric balance and a video camera, respectively. Since the experiments were conducted in nitrogen, there were no flames and the results were solely based on the condensed phase process. The results show that the sample weight loss rate of PMMA with the additives started to become slower when slight char formation was observed. The colour of PMMA with the additives became darker with time and became black after 300 s exposure. Carbonaceous char yield of the PMMA with the additives sample was about 12 % (excluding the additives left in the residue) and the peak weight loss rate of the additive sample was about 30% less than that of PMMA without the additives. As expected, no carbonaceous char was observed at the end of the test for PMMA without the additives.

The envisioned flame retardant approach is the formation of silicon-oxy-carbide (SI-O-C) type protective char by crosslinking PVA with pentacoordinate organosilicate during combustion²⁸.

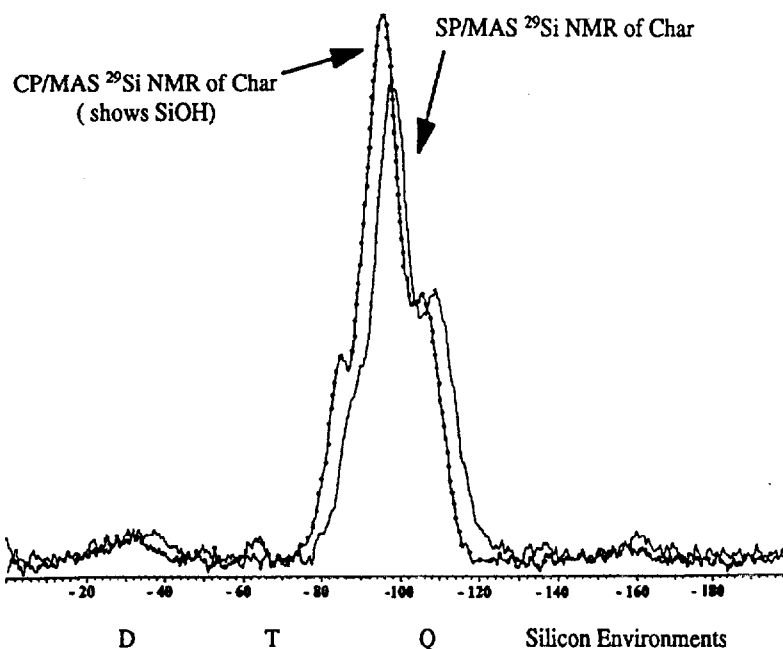


Figure 13. CP/MAS and SP/MAS ^{29}Si NMR spectra of the char from combustion in the Cone Calorimeter of PVA with silica gel/ K_2CO_3 additives (mass ratio, 90:6:4 respectively).

In order to confirm this mechanism, the char from the combustion of PVA with silica gel/ K_2CO_3 additives (mass ratio, 90:6:4 respectively) in the Cone Calorimeter was analysed using single pulse magic angle spinning (SP/MAS) ^{29}Si NMR and cross-polarisation (CP)/MAS ^{29}Si NMR which selectively enhances the signal intensities of Si nuclei near proton³⁰. Their spectrum is shown in Figure 13. The SP/MAS ^{29}Si NMR spectrum shows a broad resonance from ~ 130 ppm to ~ 90 ppm, which indicates that the char may contain some silicate species. Comparison of this spectrum to the SP/MAS ^{29}Si NMR spectrum of the char from combustion of PVA with sodium silicate (mass ratio of 90:10) confirms this possibility, since both spectra show the majority of the silicons are of the Q^3 [$(SiO)_3SiO(-)$] (100 ppm to 110 ppm) and Q^4 [$(SiO)_4Si$] (110 ppm to 120 ppm) type. The CP/MAS ^{29}Si NMR spectrum of the PVA with silica gel/ K_2CO_3 char reveals that there is still a significant fraction of Q^2 [$(SiO)_2-Si-(OH)_2$] (85 ppm to 95 ppm) and Q^3 [$(SiO)_3-Si-OH$] (95 ppm to 105 ppm) silanol functionality present after the combustion. Silanol is also present in the original silica gel structure. These spectra indicate that the majority of the silica gel original structure remains intact during the combustion and envisioned Si-O-C bonds are hardly observed in the spectra at T in the figure.

An alternative mechanism for these additives is through the formation of a potassium silicate glass as a surface barrier which insulated and slowed escape of volatile decomposition products. The latter might provide enough time for crosslinking and the formation of char among the degradation products and residues of polymer chains. At present, the flame retardant mechanism of silica gel/ K_2CO_3 additives in not only hydroxylic polymers such as PVA and cellulose but also in non-hydroxylic polymers such as PP, PS, and PMMA is not understood. We are currently working to determine the effects of particle size, internal pore size and silanol content of the silica gel on flammability properties of PP and to understand the flame retardant mechanisms.

2.3. Another Flame Retardant Approach

Another approach is the in situ formation of a barrier layer near the polymer surface during burning. An inorganic additive such as silicon based particles is dispersed into a polymer sample and accumulation of the particles to form a layer to interfere in the transport rate of the thermal degradation products of the polymer to the gas phase or to act as a thermal insulation layer.

2.3.1. Nanocomposites

2.3.1a. Experimental Study

In the pursuit of improved approaches to fire retardant polymers, a wide variety of concerns must be addressed, in addition to flammability. Generally, the addition of inorganic or organic flame retardants into polymer tends to reduce mechanical properties of the polymer. However, nylon-6 clay-nanocomposites, first developed by researchers at Toyota Central Research and Development Laboratories, were developed to have unique mechanical properties when compared to conventional filled polymers³¹. The nylon-6 clay-nanocomposites (clay mass fraction from 2% to 70%) are synthesised by ring-opening polymerization of ϵ -caprolactam in the presence of cation exchanged montmorillonite clay. This process creates a polymer layered silicate nanocomposite with either a delaminated hybrid structure (randomly dispersed silicate layers) or an intercalated hybrid structure (well ordered multilayer with spacing between the silicate layers of only a few nanometers). The mechanical properties of the nylon-6 clay-nanocomposites with 5% clay mass fraction show excellent improvement over pure nylon-6. The nanocomposite exhibits a 40% higher tensile, 68% greater tensile modulus, 60% higher flexural strength, 126 % increased flexural modulus, and comparable Izod and Charpy impact strengths. The heat distortion temperature is increased from 65 °C (nylon-6) to 152 °C (nylon-6 clay-nanocomposite)³².

To evaluate the flame retardant effectiveness of the nanocomposite approach, we have measured the flammability properties of nylon-6 delaminated clay-nanocomposites with clay mass fractions of 2% and 5%, and compared them with pure nylon-6³³. All nylon-6 clay-nanocomposites and nylon-6 were obtained from UBE industry and were used as received. The samples were prepared by compression molding into about 7.5 cm x 5 cm rectangular slab with about 1.5 cm thickness. The thermogravimetric analysis shows that there was no significant difference in weight loss rate history between nylon-6 and clay-nanocomposites with clay mass fraction of 5%³². The heat release rate curves from the Cone Calorimeter for nylon-6 and nylon-6 clay-nanocomposites (2% and 5%) when exposed to external radiant flux of 35 kW/m² are shown in Figure 14. The results show significant reduction in heat release rate and higher mass fraction of the clay reduces more heat release rate of nylon-6. Visual observation of the combustion experiments in the Cone Calorimeter reveals different behavior for the nylon-6 clay-nanocomposites compared to the pure nylon-6 from the very beginning of the thermal exposure. A thin char layer forms on the top of the all the samples in the first few

minutes of exposure prior to ignition. In the case of pure nylon-6, this char layer fractures into small pieces early during the combustion. The char does not fracture with the nylon-6 clay-nanocomposites. This tougher char layer survives and grows throughout the combustion, yielding a rigid multicellular char-brick. The nanocomposite structure appears to enhance the toughness of the char through reinforcement of char layer. The TEM of a section of the residual char from the nylon-6 clay-nanocomposite (5% mass fraction) is shown in Figure 15. A multilayered silicate structure is clearly seen, with the darker, 1 nm thick, silicate sheets forming a large array of fairly even layers. This was the primary morphology seen in the TEM of the char, however, some voids were also present. The original nylon-6 clay-nanocomposite sample is mostly the delaminated structure^{31,32}, this implies that the layered structure seen in the Figure 15 formed during combustion. The delaminated hybrid structure, which subsequently collapses during combustion, may act as an insulator and a mass transport barrier, slowing the escape of the volatile products generated as the nylon-6 decomposes. The nanocomposite's low permeability for liquids and gases may slow the transport of volatile products and also molten polymers through the nanocomposite layers to the sample surface³⁴.

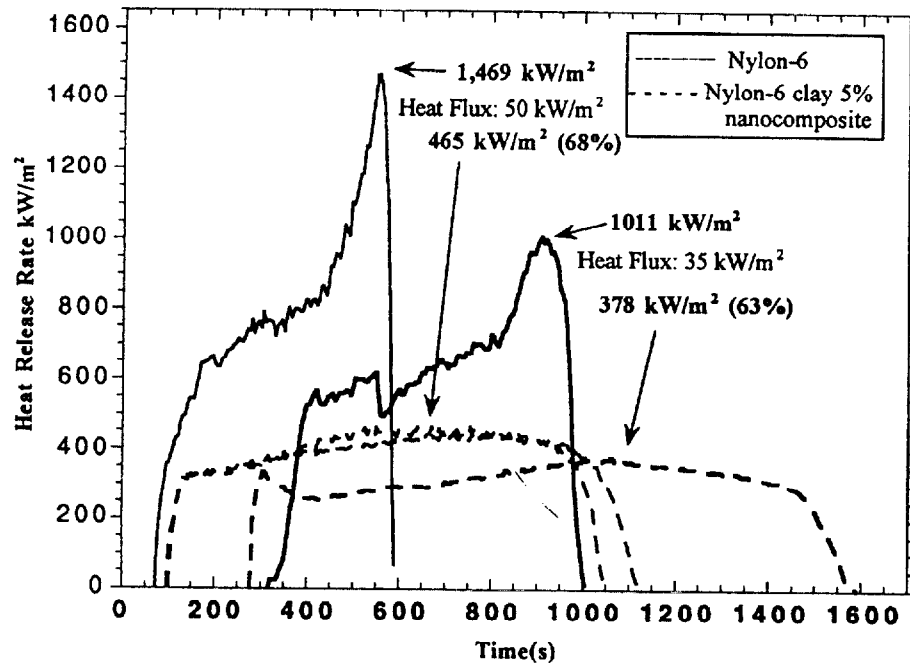


Figure 14. Comparison of heat release rate for nylon-6 and nylon-6 clay nanocomposites.

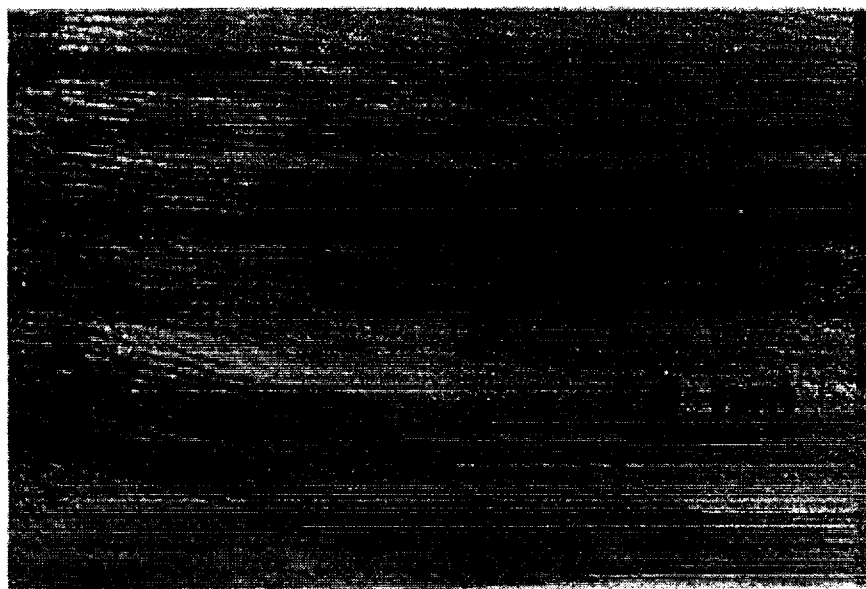


Figure 15. TEM of combustion char sample of nylon-6 clay composite.

Further X-ray and TEM analysis of the char and the original nylon-6 nanocomposite structure and gasification rate measurement of nylon-6 clay-nanocomposites in nitrogen and also in a 7% O₂/93% N₂ atmosphere without flaming in the radiative gasification apparatus are underway to better understand flammability behavior. Some new results are presented in our other paper³⁵ in this Book.

Comparison of nylon-6 clay-nanocomposites to other flame retarded nylon systems, such as the previously discussed nylon-6,6 triphenylphosphine oxide copolymer (nylon-6,6+TPO(30%)), where the flame retardant is also combined with the nylon at the molecular level, further illustrates the unique benefits the nanocomposite approach offers. Table 3 shows that the nylon-6,6+TPO(30%) copolymer gives similar reduction in heat release rate (58%) to that for the nanocomposites (63%) at a comparable level of incorporation of "flame retardants" (4% mass fraction of phosphorus). As described in the Section 2.1, the specific extinction area and CO yield (these values are normalised by mass loss rate) for the nylon-6,6 +TPO (30%) are much greater than that for the nylon-6,6. Even though the mass loss rate for the copolymer is about 50% lower than that for the nylon-6,6, the extinction by smoke is still four times greater, and the CO production rate is still 10 times greater, than that of nylon-6,6. Another additive flame retardant system for nylon, based on ammonium

polyphosphate, requires 35% mass fraction of additive to significantly effect the flammability (measured by oxygen index) of nylon-6³⁶ and this results in as much as a 20% loss of mechanical properties. Finally, it should be noted that the nano-dispersed clay composite structure has a very different effect on the flammability of nylon than macro-or meso-dispersed clay-polymer mixtures. Le Bras and Bourbigot found, in their extensive study of clays in an intumescent polypropylene system, that montmorillonite clay, similar to the ion exchanged montmorillonite clay used to make the nylon composites, actually decreased the limiting oxygen index³⁷.

Other polymer silicate nanocomposites based on a wide variety of resins such as polystyrene, epoxy, poly(ethylene oxide), polysiloxane, polyesters, and polyphosphazenes, have recently been prepared via melt intercalation^{38, 39}. These materials possess varying degrees of interaction between the polymer and the silicate layer and provide the opportunity to study the effect this variable has on flammability and to determine if the clay-nanocomposite approach is useful in reducing flammability of many polymers. We are continuing to investigate the mechanism of flame retardancy in clay and other nanocomposite materials and some of the results will be presented in our other paper in this Book.

Sample	Char Yield (%) ± 0.1	Peak HRR (Δ%) (kW/m ²) ± 15%	Mean Heat of Combustion (MJ/kg) ± 10%	Total Heat Released (MJ/m ²) ± 10%	Smoke Mean Extinction Area (m ² /kg) ± 10%	Mean CO yield (kg/kg) ± 10%
Nylon-6	0.3	1011	27	413	197	0.01
Nylon-6 clay-nanocomposite 2%	3.4	686 (32%)	27	406	271	0.01
Nylon-6 clay-nanocomposite 4%	5.5	378 (63%)	27	397	296	0.02
Nylon-6,6	0	1190	30	95	200	0.01
Nylon-6,6 -PO 4% Phosphorus	8.7	490 (58%)	18	50	1400	0.16

Table 3. Cone Calorimeter data of nylon-6,6 clay nanocomposites and nylon-6 triaryl phosphine oxide copolymer

2.3.1b. Computer Simulations

A computer program, hereafter referred to as MD_REACT, that was developed in this laboratory to study the thermal degradation of polymers⁴⁰⁻⁴³, is also being used to determine the mechanism for the increase in the thermal stability and fire resistance of polymer nanocomposites. The basis of MD_REACT is molecular dynamics. This technique consists of solving Hamilton's equations of motion for each of the 3N molecular degrees of freedom. The form of the Hamiltonian used in the calculations reported in this investigation was derived from the Consistent Valence Forcefield (CVFF) developed by Molecular Simulations, Inc. (MSI)⁴⁴. A more detailed description of the force field used in the calculations can be found elsewhere⁴³.

The unique capability of MD_REACT is that it allows for the formation of new bonds from free radical fragments generated when bonds in the polymer break and, thereby, account for the chemical reactions which play a major role in the thermal degradation process. Some of these are: bond scission, depolymerization, hydrogen transfer, chain stripping, cyclization, crosslinking and radical recombination reactions. The depolymerization and intramolecular hydrogen transfer reactions, in particular, are modelled by introducing two new atom types (cf and ccf) into the CVFF forcefield to account for beta scission. The ccf atom type corresponds to an aliphatic carbon (c) bonded to a free radical carbon (cf). Once a free radical is formed, the dissociation energies of the c-ccf and h-ccf bonds (beta to cf) are reduced by 317 kJ/mol (to 51 kJ/mol and 137 kJ/mol, respectively) which corresponds to the difference between a carbon-carbon single and double bond.

The thermal degradation experiments were performed on polypropylene/graphite, rather than nylon-6/clay nanocomposites. In making this decision, we were motivated by the considerable body of experience and high level of confidence that we have acquired in using the CVFF forcefield to model hydrocarbon polymers and surfaces and we did not want to introduce any additional ambiguities into the interpretation of the computer simulations. The model of the polymer/graphite nanocomposite consisted of 4 chains of isotactic polypropylene each containing 48 propylene monomers and a graphite sheet with about 600 carbon and 80 hydrogen (used to terminate the edges of the surface) atoms.

A series of nanocomposite structures with the polymer intercalated between graphite layers which were separated by a variable distance, b , was obtained by annealing the model polymer and graphite inside of a unit cell with the following dimensions: $a = 100$, $c = 30$ and

$b = 25, 28, 30, 32$ and 50 \AA . The same model polymer was used in all of the structures. Thus, only the distance between the graphite sheets and, consequently, the density of the composite was allowed to change from one simulation to the next. The simulated annealing was performed by heating the polymer/graphite assembly to 500 K for 100 time steps and then relaxing it by performing 100 iterations of the Polak Ribiere conjugate gradient minimization⁴⁴. The entire process was repeated until the potential energy of the fully optimized structure was lower than any of the values attained during the course of the simulated annealing procedure.

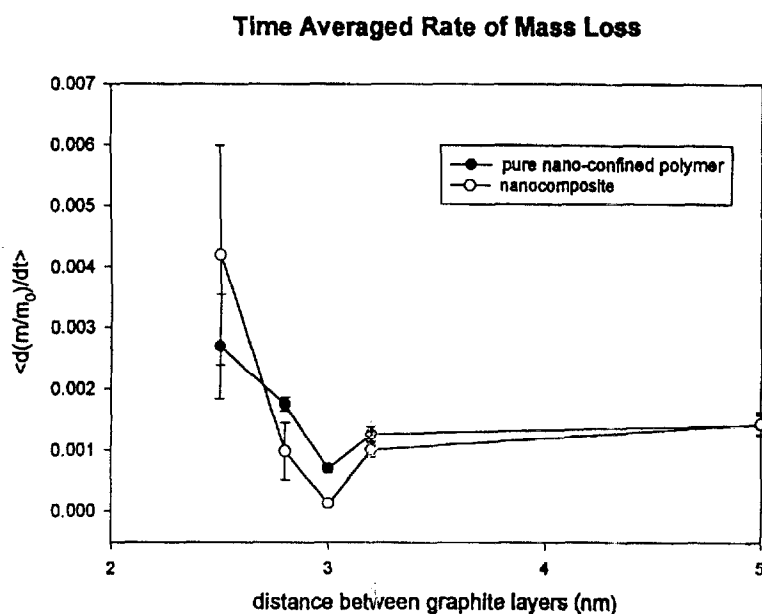


Figure 16. The effects of the separation distance between the graphite layers on the average mass loss of PP with (open circles) and without (closed circles) the interaction between the layers and the polymer.

The average rate of mass loss for both the pure nano-confined polymers and the nanocomposites are plotted as a function of the distance of separation between the graphite layers in Figure 16. The stabilization of the polymer is most pronounced in the $b = 30 \text{ \AA}$ nanocomposite and approaches zero at $b = 50 \text{ \AA}$, when the graphite layers are too far apart for there to be a significant interaction between them. At these large distances of separation, the interactions are almost exclusively between the polymer and the graphite which should

approximate what occurs in the delaminated nanocomposites where the graphite layers are individually dispersed in the polymer matrix. The observation that the thermal stability of the polymer increases when it is intercalated but is unaffected when the layers delaminate is consistent with recent experimental results that indicate that intercalated nanocomposites are more thermally stable than delaminated nanocomposites^{45,46}. Indeed it was noted that the derivative thermogravimetric (DTG) curves corresponding to the delaminated nylon-6/clay nanocomposites were almost identical to the values obtained from pure nylon-6, whereas the DTG curves of intercalated polystyrene/clay nanocomposites were shifted to dramatically higher temperatures than what was observed for pure polystyrene³⁵.

A comparison of computer animations of the trajectories, corresponding to the nanocomposites and pure nano-confined polymers, corroborate the observations we made about the effects of the interactions between the polymer and the graphite from consideration of the mass loss data. In general, the polymers in the nanocomposites lost fewer fragments and retained their shape longer than the pure nano-confined polymers. We also observed that there was a tendency for the fragments that did form to collide with the graphite surface and bounce back into the central unit cell where they could undergo recombination reactions with other free radical polymer fragments, rather than escape from the melt as combustible fuel. The last frames from the animated trajectories of the pure polymer and the $b = 30 \text{ \AA}$ nanocomposite are depicted in Figure 17. A comparison indicates that the fragments only escape from the sides of the nanocomposite (right), whereas they leave the pure nano-confined polymer from all directions (left).

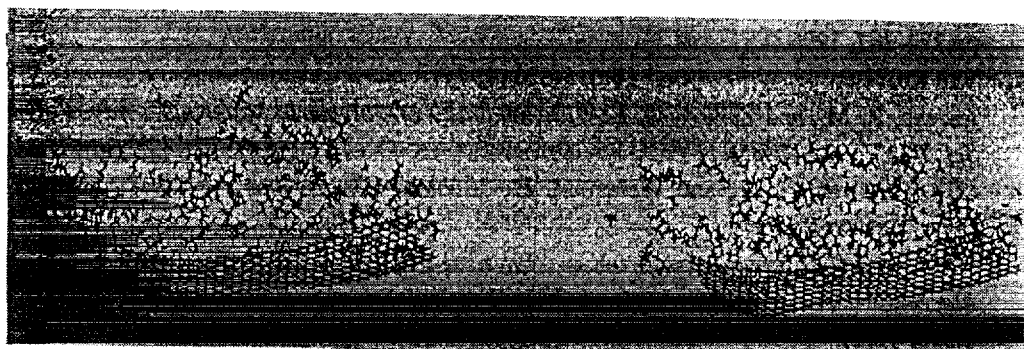


Figure 17. *Animated trajectories of polypropylene with the separation distance of 30 Å between the graphite layers, without the interaction between layers and the polymer (left), and with the interaction (right).*

3. SUMMARY

The search for new effective flame retardants is becoming more efficient due to the availability of bench scale tools such as Cone Calorimeter for the measurement of various flammability properties relevant to fire performance, and the availability of various analytical tools to determine chemical structures of polymer residues collected at various stages of pyrolysis/combustion. The development of theoretical tools such as molecular modelling is acting a guiding tool for the development of new flame retardants. Thus, new promising flame retardants such as silica gel and nanocomposites are found and their flammability properties and characteristics are described in this paper, although their retardant mechanisms have not been fully understood. Albeit the characteristics of the new flame retardants need improvement to satisfy their environmental impact, processability, and cost, we are quite optimistic that more fire safe materials will be produced with new, more efficient flame retardants.

References

1. Mita, I., "Effects of Structure on Degradation and Stability of Polymers" in *Aspects of Degradation and Stabilization of Polymers, Chapter. 6*, H.H.G. Jellinek, Ed., Elsevier Scientific, Amsterdam, 1978.
2. Kelen, T., "Polymer Degradation", Van Norstrand Reinhold, New York, 1983.
3. Grassie, N., and Scott, G., "Polymer Degradation Stabilization", Cambridge University Press, Cambridge, 1985.
4. Factor, A., "Char Formation in Aromatic Engineering Polymers", in "Fire and Polymers" (G.L. Nelson, Ed.), ACS Symposium Series 425, ACS, Washington, DC, pp.274-287, 1990.
5. Van Krevelen, D. W., *Polymer* 16:615-620 (1975).
6. Aseeva, R. M., and Zaikov, G. E., "Flammability of Polymeric Materials", *Adv. Polym. Sci.* 70:172-229 (1985).
7. Clift, R., Grace, J. R., and Weber, M. E., "Bubbles, Drops, and Particles", Academic Press, New York, 1978.
8. Matsuoka, S., and Kwei, T.K., "Physical Behavior of Macromolecules", in *Macromolecules*, F. A. Bovey and F.H. Winslow Eds., Academic Press, New York, p.346, 1979.
9. Kashiwagi, T., and Ohlemiller, T. J., *Nineteenth Symposium (International) on Combustion*, The Combustion Institute, Pittsburgh, pp.815-823 (1982).
10. Gibov, K. M., Shapovalova, L. N., and Zhubanov, B. A., *Fire Mater.* 10:133-135 (1986).

11. Hamins, A., Konishi, K., Borthwick, P., and Kashiwagi, T., *26th Symposium (Int.) on Combustion*, The Combustion Institute, Pittsburgh, pp.1429-1436 (1996).
12. Hamins, A. J., Fischer, S. J., Kashiwagi, T., Klassen, M. E., and Gore, J. P., *Combust. Sci. Tech.*, **97**:37-62 (1994).
13. Modak, A. T., *Fire Safety J.*, **3(2-4)**:177-184 (1981).
14. Nelson, G. L., "Recycling of Plastics - A New FR Challenge", *The Future of Fire Retarded Materials: Applications & Regulations*, FRCA, Lancaster, PA, p.135, 1994.
15. Van Riel, H. C. H. A., "Is There a Future in FR Material Recycling; The European Perspective", *The Future of Fire Retarded Materials: Applications & Regulations*, FRCA, Lancaster, PA, p.167, 1994.
16. Anderson, C. E., Jr., Ketchum, D. E., and Mountain, W. P., *J. Fire Science*, **6**:390-410 (1988).
17. Camino, G., Costa, L., Casorati, E., Bertelli, G., and Locatello, R., *J. Appl. Polym. Sci.*, **35**:1863-1876 (1988).
18. Scharf, D., Nalepa, R., Heflin, R., and Wusu, T., *Fire Safety J.*, **19**:103-117 (1992).
19. Weil, E. D., "Encyclopaedia of Polymer Science and Technology", Wiley-Interscience, New York, Vol.11, 1986.
20. Aaronson, A. M., "Phosphorous Chemistry", *ACS Symposium Series 486*, Chapter 17, p.218, 1992.
21. Papa, A. J., "Flame Retarding Polyurethanes" in "Flame Retardancy of Polymeric Materials" (Volume 3), Kuryla, W. C. and Papa, A. J., Eds., Marcel Dekker, New York, pp.1-133, 1975.
22. Carnahan, J., Haaf, W., Nelson, G., Lee, G., Abolins, V., and Shank, P., "Investigation into the Mechanism for Phosphorous Flame Retardancy in Engineering Plastics", "Proceeding of 4th International Conference on Fire Safety", Product Safety Corp., San Francisco, CA, 1979.
23. Smith, C. D., Gungor, A., Wood, P.A., Liptak, S. C., Grubbs, H., Yoon, T. H., and McGrath, J. E., *Makromol. Chem., Macromol. Symp.*, **74**:185 (1993).
24. Wan, I. Y., McGrath, J. E., and Kashiwagi, T., ACS Symposium Series 599, "Fire and Polymers II", edited by G. Nelson, Washington, D.C., p.29, 1995.
25. Wan, I.Y. and McGrath, J.E., *Polymer Preprints*, **36(1)**: 493 (1995).
26. Hastie, J.W. "Molecular Basis of Flame Inhibition", *J. Research of NBS-A. Physics & Chemistry*, **77A**: 733-754 (1973).
27. Hastie, J. W. and McBee, C. L., "Mechanistic Studies of Triphenylphosphine Oxide-Poly(Ethyleneterephthalate) and Related Flame Retardant Systems", NBSIR 75-741 (1975).
28. Laine, R. M., *Nature*, **353**:642 (1991).
29. Gilman, J. W., Ritchie, S. J., Kashiwagi, T., and Lomakin, S. M., *Fire and Materials*, **21**:23-32 (1997).

- 30 Gilman, J. W., Lomakin, S. M., Kashiwagi, T., VanderHart, D. L., and Nagy V., *Polymer Preprints*, **38(1)**:802-803 (1997).
- 31 Usuki, A., Kojima, Y., Kawasumi, M., Okada, A., Fukushima, Y., Kurauchi, T., and Kamigaito, O., *J. Mater. Res.*, **8**:1179 (1993).
- 32 Kojima, Y., Usuki, A., Kawasumi, M., Okada, A., Fukushima, Y., Kurauchi, T., and Kamigaito, O., *J. Mater. Res.*, **8**:1185 (1993).
- 33 Gilman, J.W. and Kashiwagi, T., *SAMPE J.*, **33**:40-46 (1997).
- 34 Giannelis, E. and Messersmith, P., *J. Polym. Sci. A: Polym. Chem.*, **33**:1047, 1995.
- 35 Gilman, J. W., Kashiwagi, T., and Lichtenhan, J. D., "Nanocomposites: A Revolutionary New Flame Retardant Approach", "Proceeding of the 6th European Meeting on Fire Retardancy of Polymeric Materials", Lille (1997).
- 36 Levchik, S., Camino, L., Costa, L., and Levchik, G., *Fire and Materials*, **19**:1 (1995).
- 37 Le Bras, M., and Bourbigot, S., *Fire and Materials*, **20**:39 (1996).
- 38 Vaia, R., Jandt, K., Kramer, E., and Giannelis, E., *Macromolecules*, **28**:8080 (1995).
- 39 Giannelis, E., *Adv. Mater.*, **8**:29 (1996).
- 40 Nyden, M. R. and Noid, D. W., *Phys. Chem.*, **95**:940 (1991).
- 41 Nyden, M. R., Forney, G. P., and Brown, J. E., *Macromolecules* **25**:1658 (1992).
- 42 Nyden, M. R., Brown, J. E. and Lomakin, S. M., *Mat. Res. Soc. Symp. Proc.*, **278**:47 (1992).
- 43 Nyden M. R., Coley, T.R., and Mumby, S., *Polym. Eng. Sci.*, **37(9)** (1997).
- 44 "Discover User Guide, Part 3", MSI, San Diego, (1995).
- 45 Lee, J., Takekoshi, T., and Giannelis, E., *Mat. Res. Soc. Symp. Proc.*, **457**:513 (1997).
- 46 Lee, J., and Giannelis, E., *Polymer Preprints*, **38**:688 (1997).

Acknowledgements

The authors are grateful to Professor J. McGrath and Dr. I. Y. Wan at Virginia Tech. for the sample preparation with phosphine oxides, Dr. Henry Yue at Dow Corning Corp. for ²⁹Si NMR analysis, Dr. C. Jackson for TEM analysis of polymer residues, Mr. Jack Lee and Michael Smith for the flammability measurements in Cone Calorimeter, and the FAA Tech. Center (Interagency Agreement DTFA003-92-Z-0018) for partial support of this Work.